EUROFUSION WPMST1-PR(16) 14709

A Gallo et al.

Effect of plasma geometry on divertor heat load spreading: simulations and experimental results from TCV.

Preprint of Paper to be submitted for publication in
22nd International Conference on Plasma Surface Interactions
in Controlled Fusion Devices (22nd PSI)

This work has been carried out within the framework of the EUROfusion Consortium and has received funding from the Euratom research and training programme 2014-2018 under grant agreement No 633053. The views and opinions expressed herein do not necessarily reflect those of the European Commission.

Effect of plasma geometry on divertor heat flux spreading: MONALISA simulations and experimental results from TCV

A. Gallo [a], N. Fedorczak [a], R. Maurizio [c], S. Elmore [b], C. Theiler [c], B. Labit [c], H. Reimerdes [c], F. Nespoli [c], P. Ghendrih [a], T. Eich [d] and the EUROfusion MST1 and TCV teams.

[a] CEA Cadarache, IRFM, F-13108 Saint-Paul-Lez-Durance, France.
[b] CCFE, Culham Science Center, Abingdon, OX14 3DB, UK.
[c] Ecole Polytechnique Fédérale de Lausanne, Swiss Plasma Center, CH-1015 Lausanne, Switzerland.
[d] Max-Planck-Institute for Plasma Physics, Boltzmannstr. 2, D-85748 Garching, Germany.

Abstract

Safe ITER operations will rely on *power spreading* to keep the *peak heat flux* within divertor material constraints. A solid understanding and parameterization of the heat flux is therefore mandatory. This paper focuses on the *separability* of the effects of plasma geometry from those of transport in divertor heat flux profiles. Numerical profiles, obtained for a broad variety of devices and magnetic equilibria with a simple model of the scrape-off layer transport called MONALISA, show agreement with a purely diffusive model for cylindrical plasmas, suggesting that geometry and transport can be easily separated. A dedicated experiment on TCV was designed to further test this assumption: L-mode plasmas with similar control parameters and shape but different divertor leg size ($Z_{mag} = -14, 0, 28\ cm$) are used to study the impact of geometry on divertor and upstream transport. Heat flux profiles, characterized with Langmuir probes and infrared thermography, exhibit unexpected behavior with the divertor leg size: the *power decay length* (λ_q) increases, while the *spreading factor* (S) shows no clear trend. These findings suggest that the link between geometry and transport is currently not yet understood and, furthermore, that upstream and divertor transport can hardly be disentangled.

1. Introduction

ITER will need to be run as close as possible to its operational limits in order to maximize fusion performance. In particular, the spreading of the heat flux on the divertor surface will set the maximum energy throughput allowed in ITER discharges within the divertor material constraint of 10 MW m^{-2} in steady state [1]. For a given input power and a given plasma geometry (divertor shape plus magnetic equilibrium), the heat flux is set by the *heat channel width*: this quantity determines the divertor wetted area and thus the footprint of the heat flux profile as well as its peak value. Experimental measurements performed on JET and ASDEX-Upgrade (AUG) [2] showed that parallel heat flux profiles at the target (${q_\parallel}^{tgt}$) are well parametrized by the convolution of a decaying exponential in the main scrape-off layer (SOL) with a further Gaussian spreading in both the main SOL and in the private flux region (PFR). The e-folding length of the exponential tail is called *power decay length* (${\lambda_q}^{tgt}$), while the width of the Gaussian is known as *spreading factor* (S^{tgt}). In order to compare different machines and extract scaling laws, it is necessary to remove the geometrical effects due to

magnetic equilibrium and to the divertor shape and tilting with respect to magnetic field lines. Target profiles are then "remapped" to a reference location, conventionally the outer midplane (OMP), accounting for the *magnetic flux expansion* (f_x), defined as the ratio of the distance between two given flux surfaces evaluated at the divertor target and at the OMP, calculated according to [3]. After such a coordinate transformation, parallel heat flux profiles at the OMP ($q_{\parallel}$) can still be parameterized in terms of the upstream scale lengths λ_q and S, which are now purged from obvious geometrical effects and embed only the information related to transport. On the one hand, λ_q is a result of the competition between parallel and perpendicular transport around the main plasma: scaling laws obtained from a multi-machine database [4] showed that λ_q depends mainly on the poloidal magnetic field at the OMP (B_P) for all devices and therefore seems to be a universal feature. Extrapolations to ITER based on this scaling law return a frighteningly small ${\lambda_q}^{ITER} \cong 1\ mm$. On the other hand, S is related to the transport in the divertor region which makes it a machine-dependent feature. For this reason a scaling law based on plasma parameters is a challenging task: in [5] it was shown that S also has a strong dependence on B_P and on the upstream electron density (n_e) or, equivalently, on the target electron temperature (${T_e}^{tgt}$), at least in JET and AUG. An increase of S was detected in AUG for the closed divertor configuration with respect to the open one, underlining its dependence on divertor specific transport mechanisms, including neutrals. It should be remembered that both λ_q and S concur to set the overall heat channel width and therefore they are equally important: for this reason it is convenient to embed them in a single quantity, the so-called *integral power decay length* (λ_{int}), which is directly linked to the peak heat flux: $q_{max} = P_{SOL}/2\pi R\lambda_{int}$. This quantity is an estimate of the heat channel width and can be easily expressed as $\lambda_{int} = \lambda_q + 1.64S$ [6]. However, since λ_q is pretty much set once a scenario is chosen under performance constraints (e.g. the 15 MA diverted H-mode in ITER), the dependence on the divertor design exhibited by S should leave some room for the possibility of reducing q_{max}. In other words, if the peak heat flux on ITER will be unacceptable, there is still a chance to reduce it by redesigning the divertor. In a similar panorama of experimental observations/extrapolations and in the absence of first-principle theoretical models for the robust prediction of the ITER heat channel width, a simple approach for the modeling of SOL transport is proposed, allowing the correlation of a few key plasma parameters to a restricted set of transport mechanisms and representing an easy way to test important, and universally accepted, assumptions on plasma geometry. In particular, a Monte Carlo code named MONALISA is used to study the separability between the effect of plasma geometry and those related to transport in numerical outer strike point (OSP) heat flux profiles. In section 2 a short description of the code is given. Section 3 discusses the effect of plasma geometry on numerical heat flux profiles and compares them with a simple theoretical model. In section 4 MONALISA simulations are compared with an experimental characterization through Langmuir probes (LP) and infrared thermography (IR) of the effect of plasma geometry on λ_q and S on TCV. Section 5 is dedicated to the discussion of results and to conclusions.

2. A simple model of SOL energy transport

MONALISA is a Monte Carlo code for the simulation of SOL energy transport and target heat flux profiles in realistic tokamak geometry but with simplified physics. It is based on

experimental magnetic flux (ψ) maps from equilibrium reconstruction codes (e.g. EFIT or LIUQE) and realistic tokamak wall contours. In simulations, energy packets are generated at a point-like source located in the confined plasma with a Maxwellian energy distribution (T) and then freely stream along magnetic field lines at constant parallel velocity ($v_{\parallel}$), thanks to a predictor/corrector scheme (order 2) with linear interpolation on the magnetic map. While doing so, they undergo homogeneous diffusion in the direction perpendicular to field lines (modeled with a homogeneous diffusion coefficient ($D_{\perp}$) over the entire plasma volume), eventually crossing the separatrix and following open field lines until the machine wall. Full curvature drifts, as well as $E \times B$ drifts (based on an *ad hoc* electric potential map), can be added to the system. When a heat packet strikes the wall, its kinetic properties ($v_{\parallel}$, $E_{\perp}$) are locally stored. By repeating the process for a high number of heat packets ($10^4 - 10^6$) in a Monte Carlo fashion and by performing local fluid interpolation on the whole wall contour, it is possible to reproduce target heat flux profiles whose shape is qualitatively consistent with those observed in experiments. It should be noted that the results don't depend on the position of the source, provided that the latter is far enough inside the separatrix to ensure that heat packets are poloidally uniformly distributed before entering the SOL. The strong points of MONALISA are its flexibility and quickness: since there's no need of a grid aligned to ψ surfaces, the code is ready to simulate any magnetic configuration (limiter, single or double null, snowflake, etc.) on any device once ψ map and wall geometry are given; it is also a fast "particle" tracer and therefore the simulation time ranges from few minutes to few hours, depending on the machine size and on the value of $D_{\perp}$. This features allow fast scans of control parameters such as I_P, T, B_T and $D_{\perp}$, as well as tuning of the drifts. Figure 1 gives an example of the typical MONALISA output: $q_{\parallel}$ profiles (only OSP is shown) for three simulations based on the same magnetic equilibrium but with different transport parameters are superimposed. Control parameters and results from the fit [2] are summarized in table 1. With respect to the reference case (blue squares, $D_{\perp} = 1\ m^2 s^{-1}$, no drifts), the addition of curvature drifts (red dots) impacts the inboard-outboard asymmetry causing a higher peak heat flux (q_{max}) since more energy reaches the OSP. On the other hand, a stronger diffusion coefficient (green diamonds, $D_{\perp} = 4\ m^2 s^{-1}$, no drifts) determines a bigger spreading in both the main SOL and PFR, so q_{max} decreases while $\lambda_q$and S increase. The dashed fitting lines are obtained following the approach described in [2] showing that the numerical profiles can be parameterized consistently with the experimental ones. Moreover, $S/\lambda_q \approx 40\%$ as found in the multi-machine database [4], suggesting that the profiles asymmetry is accurate. It has to be clarified that MONALISA shouldn't be considered as an alternative to more complex edge codes but rather as a faster and lighter complementary tool to check simple assumptions, disentangle the effect transport mechanisms and explore different (or new) configurations. Even though the physics included in the code is fairly simple compared to the complexity of experimental reality, making any attempt of quantitative estimate of q_{max} fruitless, it is worth taking advantage of the wide variety of devices and magnetic geometries that MONALISA can tackle in order to address the effect of plasma geometry on λ_q and S .

3. Effect of geometry in a purely diffusive cylindrical plasma

Taking full advantage of the speed and flexibility of MONALISA in handling different plasma geometries, a database of magnetic equilibria from AUG, TCV, WEST, JET and

COMPASS was explored, covering a wide zoology of plasma shapes and sizes ($k = 1.46 - 1.78, q_{cyl} = 1 - 10, \delta^{up} = 0.08 - 0.37, \delta^{low} = 0.28 - 0.79$). Several simulations were run for each equilibrium making a semi-random scan of the main control parameters ($I_P, B_T, D_\perp, T$) around their reference values in order to mimic the scatter of conditions typical of a real experimental database. It should be noted that, ψ maps were linearly scanned when changing I_P, neglecting variations of the Shafranov shift. For the sake of simplicity, drifts were turned off in this study. Numerical OSP heat flux profiles were then fitted according to [2] in order to extract λ_q and S. With the aim of checking whether, under the assumption of the model, remapping with f_x is indeed a robust way to remove geometrical effects, it is worth comparing MONALISA values of λ_q with those theoretically predicted for a purely diffusive cylindrical plasma, in the following way:

$$\tau_\parallel = \tau_\perp$$

$$\frac{L_\parallel}{c_s} = \frac{{\lambda_q}^2}{D_\perp}$$

$${\lambda_q}^{Theo} = \sqrt{D_\perp \frac{L_\parallel}{c_s}} = \sqrt{D_\perp \frac{\pi\, R\, q_{cyl}}{c_s}}$$

$$q_{cyl} = \frac{a}{R}\frac{B_T}{B_P}\frac{1+k^2}{2}$$

Here $\tau_\parallel$ and $\tau_\perp$ are the parallel and perpendicular transit times, $L_\parallel$ is the parallel connection length, q_{cyl} is the cylindrical safety factor (not to be confused with the heat flux, also labeled with the letter q), a and R are minor and major radius, while k is the plasma elongation. Comparison is made in figure 2, where numerical values (${\lambda_q}^{Mona}$) are plotted against ${\lambda_q}^{Theo}$ calculated for the corresponding magnetic equilibrium and using the same $D_\perp$ value. For the entire database points fall on the same straight line meaning that, regardless the device and the magnetic equilibrium, ${\lambda_q}^{Mona}$ is always a constant fraction of ${\lambda_q}^{Theo}$, within Monte Carlo fluctuations. This result proves that ${\lambda_q}^{Theo}$, which embeds q_{cyl} and thus the rough approximation of a cylindrical plasma shape, is a good proxy for MONALISA profiles: once heat flux profiles are remapped at the OMP, all equilibria behave the same way, leading to the conclusion that the geometrical information is efficiently dropped together with f_x. An example is shown in figure 3a, where two TCV equilibria with same upstream plasma shape but different divertor leg size are considered: the $L_\parallel$ (from OMP to outer target) for the plasma at the bottom (blue) is in the order of 10 m, while for the one at the top (red) it is about twice. Based on the abovementioned square root dependence of λ_q on $L_\parallel$, a factor of 2 increase ($\Delta L_\parallel \sim 100\%$) should lead to a 40% increase in λ_q. Instead, MONALISA simulations based on the two equilibria show a difference in λ_q lower than 5%. This can be understood by detailing the buildup of λ_q along the path from the OMP to the target, in terms of local diffusion steps in the radial direction:

$$dr_{loc}{}^2 = D_\perp t$$

$$dr^2 \equiv \frac{1}{f_{x\,loc}{}^2}\, dr_{loc}{}^2 = \frac{1}{f_x{}^2}\, D_\perp\, \frac{dL_\parallel}{v_\parallel}$$

$$\lambda_q{}^2 = \int_{omp}^{tgt} dr^2 = \frac{D_\perp}{v_\parallel} \int_{omp}^{tgt} \frac{dL_\parallel}{f_x{}^2} \equiv \frac{D_\perp}{v_\parallel}\, L_\parallel{}^{eff}$$

$$L_\parallel{}^{eff} = \frac{L_\parallel}{\langle f_x{}^2 \rangle}$$

where $f_{x\,loc}$ is the local flux expansion with respect to the OMP and $\langle f_x \rangle$ is the average of the same quantity over the whole $L_\parallel$. In other words, diffusion steps in the radial direction taking place in the region below the X-point are less effective in broadening $q_\parallel$ profiles because of the higher flux expansion, as can be seen in the map of figure 3b. When weighted by $\langle f_x{}^2 \rangle$, different portions of $L_\parallel$ don't matter equivalently:

$$L_\parallel{}^{eff} = \frac{L_\parallel{}^{upstr}}{\left(f_x{}^{upstr}\right)^2} + \frac{L_\parallel{}^{div\ leg}}{\left(f_x{}^{div\ leg}\right)^2} \approx \frac{10\ m}{1} + \frac{10\ m}{3^2} \approx 11\ m$$

Therefore a factor of ~ 2 difference in $L_\parallel$, as for the two cases in figure 3a ($\Delta L_\parallel \sim 100\%$), corresponds to a $\Delta L_\parallel{}^{eff} = 10\%$ only, coherent with the $\Delta\lambda_q \sim 5\%$ found by MONALISA. This reasoning, valid for a purely diffusive system, supports the idea that λ_q, set by control parameters where f_x is small (upstream), contains only the information related to transport disentangled from geometry. Once the separability of geometry and transport effects is verified in a simplified model, these assumptions have to be tested in experimental conditions. Furthermore, the interplay between divertor and upstream transport has to be carefully investigated.

4. Experimental data from TCV: scan of plasma vertical position

To further check the separability of geometrical and transport effects, to study whether upstream and divertor transport can be disentangled and to test the simple assumptions made so far, MONALISA results will be compared with recent experimental findings from TCV. Under the flagship of the EUROfusion MST1 campaign, a dedicated experiment is currently being carried out with the goal of studying the effect of the outer divertor leg size on OSP heat flux profiles and thus on transport, thanks to the shaping capabilities of TCV. Ohmic heated, low density, L-mod plasmas within the same range of control parameters ($I_P = 210\ kA, B_T = 1.4\ T, q_{95} = 4, k = 1.6$) and very similar shape of the confined region were achieved at different vertical positions of the magnetic axis (Z_{mag}), changing the size of the outer divertor leg and therefore $L_\parallel$. Three main Z_{mag} positions were explored: -14 cm (bottom), 0 cm (middle) and 28 cm (top) to which correspond $L_\parallel$ values of 12 m, 14 m, and 20 m respectively (distance along field lines from OMP to target, averaged over the whole

SOL). Experimental conditions for the considered database, as well as shot numbers, are summarized in table 2. The characterization of outer divertor heat flux profiles is performed with Langmuir probes (LP) and infrared thermography (IR). All the shots were performed in steady state conditions: during the first part of the shot the OSP was kept at constant position for better IR measurements, while during the second it was swept (2 cm / 300 ms) to increase LP spatial coverage. The LP setup of TCV consists of 26 probes distributed along the floor of the machine: the spatial resolution is 11 mm and I-V characteristics are acquired every 1.4 ms. More details about the LPs setup can be found in [7]. The recently upgraded infrared system of TCV consists of two IR cameras. The first, a Thermosensorik CMT 256M HS, is mounted on the top of the vacuum vessel and images the floor, where usually the OSP of a single-null diverted plasma sits: the spatial resolution is 2.5 mm and the typical acquisition frequency is 400 Hz in full-frame (up to 15 kHz in subframe mode). The second camera, a Equus 81k M MWIR, monitors a portion of TCV central column and can be moved between a lower port and a midplane port intra-shots, according to the expected position of the inner strike point; the field-of-view can be increased by changing lens (two lenses, with 12.5 mm and 25mm focal length, are available), corresponding to a spatial resolution of 0.8 mm and 1.6 mm respectively, while a typical acquisition rate is 200 Hz in full frame. The main deliverables of the experiment are the scale lengths λ_q and S as a function of Z_{mag}. As show in figure 4a, both LP (blue dots) and IR (red stars) show an increase of $\lambda_q$with Z_{mag} with a factor of two difference between top and bottom positions. In other words the plasma shape, in particular the divertor region, impacts λ_q: this effect cannot be captured by current scaling laws and is counterintuitive with respect to the idea of a multi-machine database [4]. This unexpected trend is not reproduced by MONALISA simulations based on the corresponding ψ maps ($D_\perp = 1\ m^2 s^{-1}$, $T_e = 50\ eV$, $curvB\ drifts$), which yield an almost constant λ_q for the three vertical positions (black squares and dashed lines in figure 3a). This discrepancy suggest that a purely diffusive model including full curvature drifts is not enough to capture non-trivial effects of plasma geometry on heat flux profiles. An important role could be played by $E \times B$ drifts and therefore this mechanism will undergo detailed investigation in future studies. More importantly, the f_x assumption (discussed in section 3), doesn't hold against the experimental evidence brought by TCV: a divertor-leg-dependent λ_q implies that, at least for these extremely spread configurations, the information related to transport cannot be separated from geometry. This "hidden" geometrical effect could be a game changer when making predictions of λ_q for future devices such as ITER, it has to be understood and will be object of further studies. On the other hand, as shown in figure 4b, no clear trend of S as a function of Z_{mag} was detected by either of the two diagnostics. This second result is also quite surprising: a spreading factor which is insensitive to the size of the divertor leg would go against the current understanding of S as related to diffusion in the PFR volume (and main SOL) along the path from the X-point to the target and thus strongly dependent on the divertor shape. Coherently with this way of thinking, MONALISA simulations exhibit increasing S with Z_{mag}. Nevertheless, as far as S is concerned, measurements should be considered cautiously: errorbars are big, as well as the scatter among the data points, with a measured quantity as small as fractions of a millimeter. This makes the analysis and the fitting of the data challenging, especially for LPs which have a smaller spatial resolution. The judgement on the behavior of the spreading factor is then suspended until future investigations. Moreover, the inner strike point heat flux profiles need to be analyzed together

with measurements of the radiated power in order to make a global power balance to ensure that the divertor plasma is kept in a similar regime across the Z_{mag} scan.

5. Discussion and conclusions

This contribution focuses on the impact of plasma geometry on OSP heat flux profiles and, in particular, on the heat channel width: this quantity depends on both the e-folding length λ_q and the spreading factor S, therefore any attempt to make meaningful predictions for ITER must take into account both of these parameters. The separability of features related to plasma geometry from the signature of transport in heat flux profiles is investigated by comparing the results of a Monte Carlo simple model of SOL transport (MONALISA) with theoretical predictions for a purely diffusive cylindrical plasma. For a number of devices and magnetic equilibria, providing a broad variety of shapes, the agreement between simulations and theory suggests that remapping at the OMP through fx is an effective way to purge λ_q from obvious geometrical details such as the divertor shape and the magnetic expansion, and thus geometry and transport can easily be disentangled. This finding supports the idea that, under the simplified assumptions of MONALISA, λ_q is set upstream and is a universal feature which depends only on control parameters, rather than plasma shape. Numerical simulation with the more sophisticated SOLEDGE2D code will be performed to further test these assumptions. Experimental measurements are currently being performed in TCV on plasmas with the same shape and control parameters but different divertor leg size with the aim of studying the interplay between upstream and divertor transport. Data from LP and IR are in good agreement and show an increasing trend for λ_q with Z_{mag} proving that, even after remapping, divertor geometry still plays an important role and, moreover, that upstream transport is impacted by the transport in the divertor region, which is a machine-specific feature. No clear trend of S was detected by either diagnostic: this is an even more striking result, suggesting the counterintuitive conclusion that the transport in the divertor is not influenced by its shape. Given the small values of S and the comparatively big errorbars, any conclusion on S is left to further investigations. This study should raise two main concerns: the first one is about the robustness of the assumption that f_x is a sufficient tool to completely take geometry out of the equation; the second one is the complex interplay between transport around the main plasma and transport in the divertor region. The answer to these questions, together with refined measurements and a better understanding of the spreading factor, are essential steps towards a sustainable handling of the ITER divertor.

Acknowledgements

This work has been carried out within the framework of the EUROfusion Consortium and has received funding from the Euratom research and training programme 2014-2018 under grant agreement No 633053. The views and opinions expressed herein do not necessarily reflect those of the European Commission.

References

[1] A. Loarte, et al., Nucl. Fusion S203-S263 (2007) 47.

[2] T. Eich, et al., Phys. Rev. Lett. 215001 (2011) 107.

[3] A. Loarte, et al., J. Nucl, Mater. 266-269 (1999) 587-592.

[4] T. Eich, et al., Nucl. Fusion 093031 (2013) 53.

[5] A. Scarabosio, et al., J. Nucl. Mater. 49-54 (2015) 463.

[6] M. A. Makowski, et al., Phys. Plasmas 056122 (2012) 19.

[7] R. Pitts, et al., Nucl. Fusion 1145-1166 (2003) 43.

Tables

Simulation	$D_\perp(m^2s^{-1})$	$curvB$ drift	$E \times B$ drift	q_{max} (a.u.)	$\lambda_q\ (mm)$	$S\ (mm)$
0211	1	0	0	$1.75 * 10^9$	4.63	1.82
0214	1	1	0	$1.35 * 10^9$	4.61	1.74
0219	4	0	0	$7 * 10^8$	8.43	3.83

Table 1: control parameters of MONALISA simulations in figure 1 and results of the fit [2]. For all cases $I_p = 210\ kA, B_T = 1.4\ T, T_{sep} = 100\ eV, \psi$ from TCV #51262 at $t = 0.7\ s$.

Z_{mag}	f_x^{tgt}	$n_{e\ av}\ (m^{-3})$	Shot numbers
$-14\ cm$	3.4	$2.5 – 2.9 * 10^{19}$	51258, 51260, 51262
$0\ cm$	2.4	$2.6 – 3 * 10^{19}$	51279, 51332, 51333
$28\ cm$	3.7	$2.8 – 3.3 * 10^{19}$	51323, 51324, 51325

Table 2: summary of experimental conditions of considered TCV database. All the shots were in L-mode, ohmic heating, $I_P = 210\ kA, B_T = 1.4\ T, q_{95} = 4, k = 1.6$.

Figures

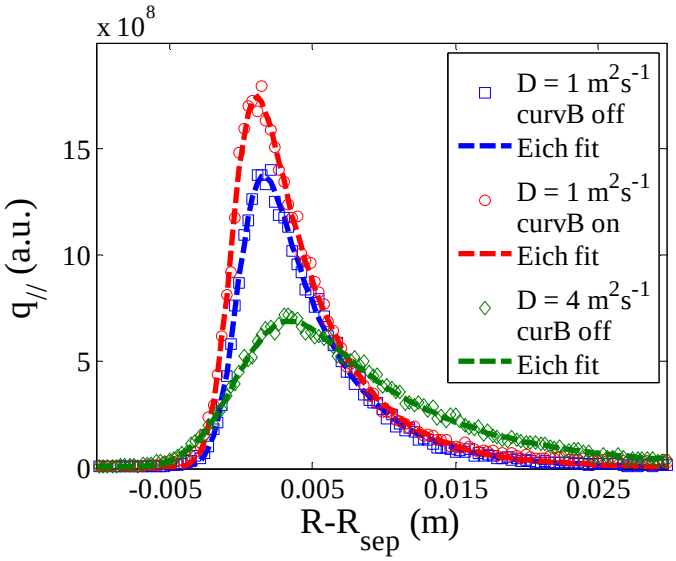

Figure 1: Example of output of MONALISA simulations. OSP parallel heat flux profiles remapped at the OMP (same magnetic equilibrium, different transport parameters).

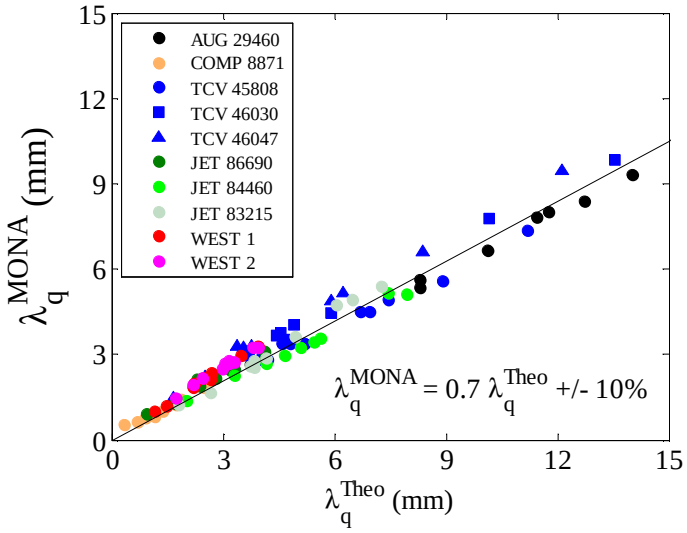

Figure 2: λ_q values from multi-machine database obtained fitting MONALISA numerical profiles plotted as a function of the value theoretically predicted for a purely diffusive cylindrical plasma.

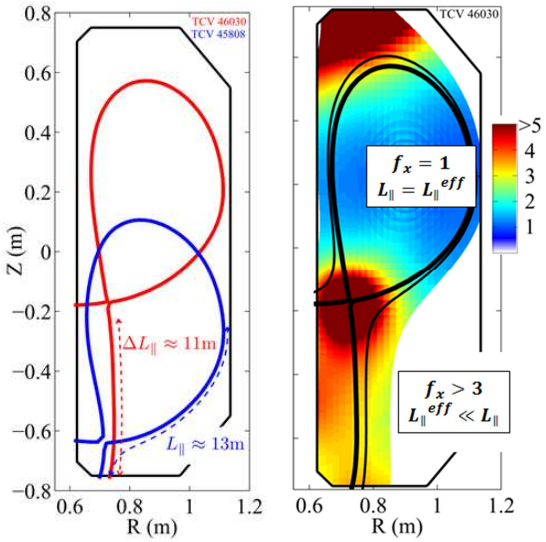

a) b)

Figure 3: a) solid lines: separatrix and parallel connection lengths of two TCV equilibria with different divertor leg size. b) flux expansion map for a TCV reference equilibrium.

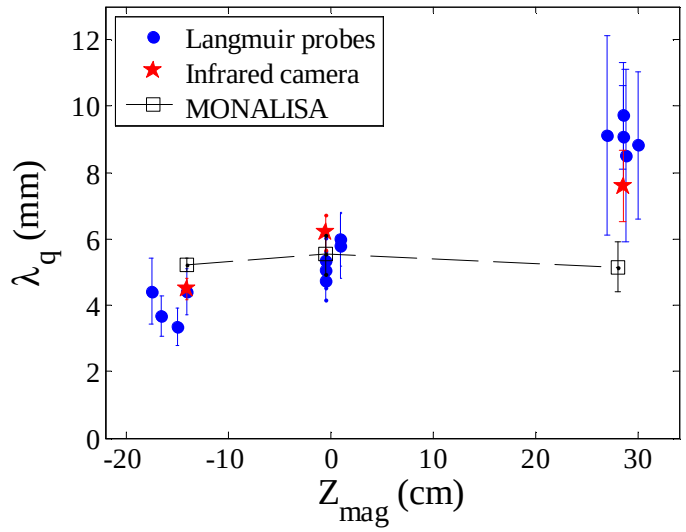

a)

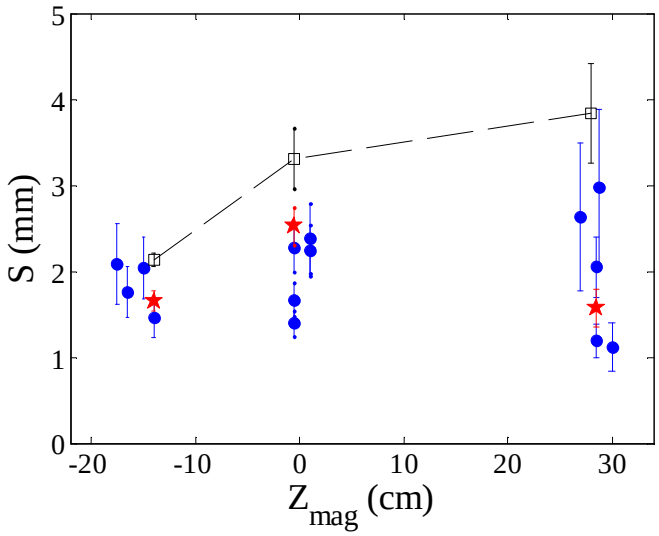

b)

Figure 4: Experimental results from TCV of λ_q (a) and S (b) as a function of Z_{mag} (blue dots for LP, red stars for IR). Black squares with dashed lines show the trends predicted by MONALISA.